

Jet cross sections with CoLoRFuINNLO

Adam Kardos*[†], Gábor Somogyi and Zoltán Trócsányi

University of Debrecen, MTA-DE Particle Physics Research Group

E-mail: kardos.adam@science.unideb.hu

We report on an automatic framework capable of calculating fully differential cross sections in QCD up to NNLO accuracy for colorless initial states. The capabilities of this program are demonstrated on three-jet production in electron-positron annihilation for which previously known event shape observables are recomputed for comparison with other calculations and NNLO QCD prediction is made for the first time for jet cone energy fraction.

Loops and Legs in Quantum Field Theory

24-29 April 2016

Leipzig, Germany

*Speaker.

[†]This research was supported by the Hungarian Scientific Research Fund grant K-101482, the Post Doctoral Fellowship programme of the Hungarian Academy of Sciences and the Research Funding Program ARISTEIA, HOCTools (co-financed by the European Union (European Social Fund ESF) and Greek national funds through the Operational Program "Education and Lifelong Learning" of the National Strategic Reference Framework (NSRF)).

1. Introduction

The strong coupling is a fundamental quantity of the standard model and QCD. Its precise measurement serves as a cornerstone of experimental high energy physics. One possible way to extract it is from event shape variables measured in electron-positron annihilation. For this high precision theoretical predictions are instrumental setting high demand on the numerical quality and accuracy of theoretical computations. Since in high energy particle physics the computational toolbox is perturbative quantum field theory the accuracy of predictions is meant to be understood as including as many terms in the perturbative expansion as possible. To use these predictions in experimental fitting procedures to extract the coupling good numerical convergence and low statistical uncertainties are required hence the demand for numerical quality.

Electron-positron annihilation can also be used as a testbed for deploying new computational methods since the initial state does not contain any colored particle thus QCD radiation can only come from colored particles in the final state. In leptoproduction state-of-the-art computations include up to seven jets [1] at NLO while up to three jets [2, 3] at NNLO accuracy. Here we apply the CoLoRFulNNLO method [4, 5], developed to compute NNLO QCD corrections for colorless initial states, we decided to apply it to three-jet production in electron-positron annihilation. This choice is also motivated by a possible strong coupling measurement on the premise that the devised method can provide predictions with numerical quality suitable for extracting the value of strong coupling or using the method to calculate new event shape observables for which no NNLO QCD prediction was available in the past and possibly finding one for which hadronization corrections are moderate making it a good candidate for strong coupling determination.

In a very early stage of creating the numerical code implementing the CoLoRFulNNLO method for three-jet production it was realized that the organization of the subtraction terms to regularize kinematic singularities is a major bookkeeping problem but with some effort it can be automated and made general. Hence we decided not to build a numerical code for three-jet production but instead a complete framework which uses the CoLoRFulNNLO method for computations in QCD up to NNLO which is user-friendly and flexible to suit user and future needs.

2. Method

The CoLoRFulNNLO method is a completely local subtraction scheme to compute jet cross sections in perturbative QCD up to NNLO accuracy, fully worked out for non-colored initial states. As any other subtraction method it relies upon adding and subtracting zero in a clever way from various contributions of the cross section. The total cross section in perturbation theory up to the NNLO correction can be written in the form of:

$$\sigma_{\text{NNLO}} = \sigma^{\text{LO}} + \sigma^{\text{NLO}} + \sigma^{\text{NNLO}}, \quad (2.1)$$

where

$$\sigma^{\text{LO}} = \int_m d\sigma^{\text{B}} J_m \quad (2.2)$$

is the LO cross section defined by the fully differential Born cross section of m final state partons and the jet function J which takes the value of J_m on the m -parton phase space. The NLO

contribution can be formally written as

$$\sigma^{\text{NLO}} = \int_{m+1} d\sigma_{m+1}^{\text{R}} J_{m+1} + \int_m d\sigma_m^{\text{V}} J_m, \quad (2.3)$$

where the sum is finite for all infrared-safe observables due to the KLN theorem. Our aim is to be able to compute fully differential cross sections thus we would like to perform all integrals in $d = 4$ dimensions numerically. To do so the two contributions have to be made separately finite which is achieved by subtracting kinematic singularities and adding them back integrated over the unresolved regions of phase space (denoted by \int_1):

$$\sigma^{\text{NLO}} = \int_{m+1} \left[d\sigma_{m+1}^{\text{R}} J_{m+1} - d\sigma_{m+1}^{\text{R},A_1} J_m \right]_{\varepsilon=0} + \int_m \left[d\sigma_m^{\text{V}} + \int_1 d\sigma_{m+1}^{\text{R},A_1} \right]_{\varepsilon=0} J_m. \quad (2.4)$$

In the case of the NLO correction only two contributions are present: the real one, with one extra parton in the final state and the virtual one, with one parton virtually exchanged, or equivalently the $(m+1)$ - and m -parton contributions. The NNLO correction is composed of three contributions:

$$\sigma^{\text{NNLO}} = \sigma_m^{\text{NNLO}} + \sigma_{m+1}^{\text{NNLO}} + \sigma_{m+2}^{\text{NNLO}} = \int_{m+2} d\sigma_{m+2}^{\text{RR}} J_{m+2} + \int_{m+1} d\sigma_{m+1}^{\text{RV}} J_{m+1} + \int_m d\sigma_m^{\text{VV}} J_m, \quad (2.5)$$

where the individual contributions are infinite, only their sum is finite for IR-safe observables. The $(m+2)$ -parton contribution contains an $(m+2)$ -parton tree-level squared matrix element which can develop kinematic singularities due to singly and doubly unresolved parton emissions. The $(m+1)$ -parton contribution is the interference of an $(m+1)$ -parton one-loop amplitude with the corresponding tree-level one exhibiting kinematic singularities due to singly unresolved emissions and explicit ε poles due to the integration over loop momentum. Finally, the m -parton contribution is the sum of the modulus squared one-loop and the interference of the two-loop amplitude with the corresponding m -parton tree-level matrix element. This last contribution does not contain any kinematic singularity, but has ε poles due to dimensional regularization of matrix elements which are cancelled by the $(m+1)$ - and $(m+2)$ -parton contributions when summed up providing a finite prediction for all IR-safe observables.

In the $(m+2)$ -parton contribution the jet function allows for up to doubly unresolved emissions hence local subtractions have to be included for both the singly ($d\sigma_{m+2}^{\text{RR},A_1}$) and doubly ($d\sigma_{m+2}^{\text{RR},A_2}$) unresolved emissions. Beside of these the subtraction terms have additional kinematic singularities: when a singly unresolved emission takes place a part of those subtraction terms which were included for the doubly unresolved emission develops kinematic singularities, while in the case of a doubly unresolved emission a subset of subtraction terms for regularizing singly unresolved emissions develops kinematic singularities. To cancel these singularities additional subtraction terms are introduced ($d\sigma_{m+2}^{\text{RR},A_{12}}$). When these kinematic singularities are regularized the $(m+2)$ -parton contribution becomes finite even in $d = 4$ dimension and has the form

$$\sigma_{m+2}^{\text{NNLO}} = \int_{m+2} \left\{ d\sigma_{m+2}^{\text{RR}} J_{m+2} - d\sigma_{m+2}^{\text{RR},A_2} J_m - \left[d\sigma_{m+2}^{\text{RR},A_1} J_{m+1} - d\sigma_{m+2}^{\text{RR},A_{12}} J_m \right] \right\}_{\varepsilon=0}. \quad (2.6)$$

The kinematic singularities of the $(m+1)$ -parton contribution are regularized by introducing appropriate subtraction terms ($d\sigma_{m+1}^{\text{RV},A_1}$), while the explicit poles are cancelled by adding back the integrated $d\sigma_{m+2}^{\text{RR},A_1}$ subtractions. These integrated subtraction terms still contain a one parton degree

of freedom which can become unresolved hence a subtraction is introduced, $\left(\left(\int_1 d\sigma_{m+2}^{\text{RR},A_1}\right)^{A_1}\right)$, to regularize these kinematic singularities. The regularized $(m+1)$ -parton contribution can be cast into the form of

$$\sigma_{m+1}^{\text{NNLO}} = \int_{m+1} \left\{ \left(d\sigma_{m+1}^{\text{RV}} + \int_1 d\sigma_{m+2}^{\text{RR},A_1} \right) J_{m+1} - \left[d\sigma_{m+1}^{\text{RV},A_1} + \left(\int_1 d\sigma_{m+2}^{\text{RR},A_1} \right)^{A_1} \right] J_m \right\}_{\varepsilon=0}. \quad (2.7)$$

After integrating over degrees of freedom of unresolved emissions in the subtractions they are added back in the last contribution, namely in the m -parton one:

$$\sigma_m^{\text{NNLO}} = \int_m \left\{ d\sigma_m^{\text{VV}} + \int_2 \left[d\sigma_{m+2}^{\text{RR},A_2} - d\sigma_{m+2}^{\text{RR},A_{12}} \right] + \int_1 \left[d\sigma_{m+1}^{\text{RV},A_1} + \left(\int_1 d\sigma_{m+2}^{\text{RR},A_1} \right)^{A_1} \right] \right\}_{\varepsilon=0} J_m. \quad (2.8)$$

Since both the $(m+2)$ - and $(m+1)$ -parton contributions are regularized by the various subtractions, due to the KLN theorem the last m -parton one has to be finite as well, the integrated subtractions cancel the explicit ε poles of the $d\sigma^{\text{VV}}$ contribution.

3. The MCCSM framework

As discussed in the previous section that the NNLO correction is composed of three different contributions, two out of these need subtractions to regularize kinematic singularities. The presence of subtractions results in the proliferation of contributions needed for the cross section turning the computation into a heavy bookkeeping problem. Since the way subtractions are assigned to singular regions is an algorithmically well-defined problem it can be automated. Having an implementation which can automatically assign subtraction terms to a partonic subprocess pays off because of the large number of these terms not only is the manual implementation cumbersome but it is not free from possible human errors. Beside the possibility to automate subtractions the other good reason for a general NNLO QCD framework is that the CoLoRFulNNLO method only needs the various squared matrix elements as input.

As for a Monte Carlo integrator the user can select from several being available in the literature [6, 7, 8, 9, 10, 11]. If the integrator is only defined on the hypercube of unity a mapping is needed from the hypercube of unity of integration to the actual physical phase space. This can also be done in an automatic way paving the road further for automation.

These properties allowed us to create the MCCSM (Monte Carlo implementing the CoLoRFulNNLO Subtraction Method) numerical code in a flexible `fortran90` program library.

3.1 Setup and initialization

MCCSM is constructed to be fully modular: each process resides in a separate folder. If NNLO QCD predictions are to be computed for a particular process the code has to be compiled in the folder of the process. The user has to provide various tree-level, one- and two-loop squared matrix elements to build a complete code, Tab. (1) gives a summary of the squared matrix elements requested by the program.

# of loops \ # of partons	m	$m + 1$	$m + 2$
0	$\mathcal{B}, \mathcal{B}_{ij}, \mathcal{B}_{ijk}, \mathcal{B}_{ijkl}$ $\mathcal{B}^{\mu\nu}, \mathcal{B}_{ij}^{\mu\nu}, \mathcal{B}^{\alpha\beta\mu\nu}$	$\mathcal{R}, \mathcal{R}_{ij}, \mathcal{R}^{\mu\nu}$	$\mathcal{R}\mathcal{R}$
1	$\mathcal{V}, \mathcal{V}_{ij}, \mathcal{V}^{\mu\nu}$	$\mathcal{R}\mathcal{V}$	
2	$\mathcal{V}\mathcal{V}$		

Table 1: Collection of user-provided matrix elements needed by MCCSM. Latin indices stand for color while greek indices for spin degrees of freedom for the color- and spin-correlated squared matrix elements.

The behavior of the code can be controlled and even fine-tuned via an input card which not only specifies the physical and Monte Carlo integrator related parameters but can also be used to fine-tune the run by selecting only specific contributions or even turning off subtraction terms to obtain NLO QCD corrections to the $(m + 1)$ -parton process.

Upon initialization MCCSM determines the partonic subprocesses of the process and the number of massless quark flavors. Then for every active contribution the squared matrix elements are evaluated in randomly chosen phase space points and the code tries to identify numerical relations between the various contributions coming from different subprocesses. For example, $e^+ e^- \rightarrow u \bar{u} g$ and $e^+ e^- \rightarrow d \bar{d} g$ differ only by a factor of four at tree-level. By identifying these relations the code can limit the calls to the matrix elements to an absolute minimum gaining considerable speed for complex multi-leg processes.

Then the code determines the subtraction terms for the irreducible subprocesses and checks limiting behavior for each one of them. With the irreducible subprocesses determined the program is ready to perform the Monte Carlo integration of the active contributions.

3.2 Obtaining the various contributions

The current version of MCCSM uses MINT [9] as the integrator. The code communicates with the integrator through interface routines residing in a module making a possible change in the integrator straightforward.

We use MINT as our integrator since it provides excellent control over the integration and offers the possibility to perform the integration grid optimization in a parallel fashion by running the code in multiple copies with differently chosen random seeds and at the end of the runs collecting all information from the runs to refine the integration grid. Using this approach no communication is needed between the various concurrently running jobs. The behavior of the code is just the same on a multi-hundred core cluster as on a desktop with multiple cores.

MINT is a Monte Carlo integrator on the hypercube of unity. To obtain a physical phase space point a mapping has to be defined which is provided by PHASER, an in-house multi-channel phase space generator.

4. Predictions

Two- and three-jet production in electron-positron annihilation were the first processes implemented in MCCSM. For these the NNLO QCD corrections are already known [2, 3] thus offering

	B	V	R	VV	RV	RR
# of PS points	100M	100M	100M	10M	10M	10M
Timing	12min	8h 17min	3h 24min	7h 32min	21h 53min	5h 26min

Table 2: Typical CPU timing for the various contributions to three-jet leptoproduction on a Intel(R) Xeon(R) E5-2695 v2 2.40GHz CPU.

the possibility to validate our calculation by comparison to existing predictions.

In electron-positron annihilation it is usual practice to give predictions for a generic O event shape observable normalized to the LO cross section for $e^+e^- \rightarrow$ hadrons, σ_0 ,

$$\frac{1}{\sigma_0} \frac{d\sigma}{dO} = \frac{\alpha_s}{2\pi} A(O) + \left(\frac{\alpha_s}{2\pi}\right)^2 B(O) + \left(\frac{\alpha_s}{2\pi}\right)^3 C(O) + \mathcal{O}(\alpha_s^4), \quad (4.1)$$

where $A(O)$, $B(O)$ and $C(O)$ are the differential cross section contributions at LO, NLO and NNLO accuracy, respectively.

For comparison with existing calculations [2, 3] we computed the six standard event shape variables: thrust, heavy-jet mass, total- and wide-jet broadening, C-parameter and the 3-to-2 jet transition variable. By way of illustration, we show our predictions for B_W and heavy-jet mass in Fig. (1). On the lower panels showing the physical predictions the band corresponds to the scale uncertainty at NNLO obtained by varying the renormalization scale between $\sqrt{Q^2}/2$ and $2\sqrt{Q^2}$. On the plots for the C -coefficient the bands correspond to the statistical uncertainty of our numerical integration. Our statistical uncertainty enlarges resulting in the opening of the band when the prediction in the bin approaches zero. On the lower panels both in the physical predictions and both on the plots for the C -coefficient the markers stand for the ratio of the other two computations compared to ours while the error bars indicating their statistical uncertainty only. From these plots it is visible that the agreement between our calculation and [3] is excellent¹, while the agreement with [2] is fairly good. We note that the comparison to [2] is hampered by the somewhat large uncertainties of that calculation. The discrepancies visible for large values of the event shapes can be attributed to statistical underestimation in the other two calculations because in the region of phase space in question (beyond the LO kinematic limits of the observables) we checked our predictions with MadGraph5_aMC@NLO [12] and found perfect agreement.

Beside the usual event shapes we also computed the NNLO QCD correction for jet cone energy fraction [13] for the first time for which the physical prediction and the NNLO QCD correction is depicted on Fig. (2).

The performance of MCCSM for this process is summarized in Tab. (2).

5. Conclusions

In this talk we introduced our numerical code, MCCSM which uses the CoLoRFulNNLO subtraction method to provide NNLO QCD corrections to three-jet leptoproduction. With our code we made predictions for event shape variables which are already known at NNLO QCD accuracy as well as presented predictions for the jet cone energy fraction for the first time at this accuracy.

¹We are grateful to S. Weinzierl for providing us with updated predictions from the code of ref. [3].

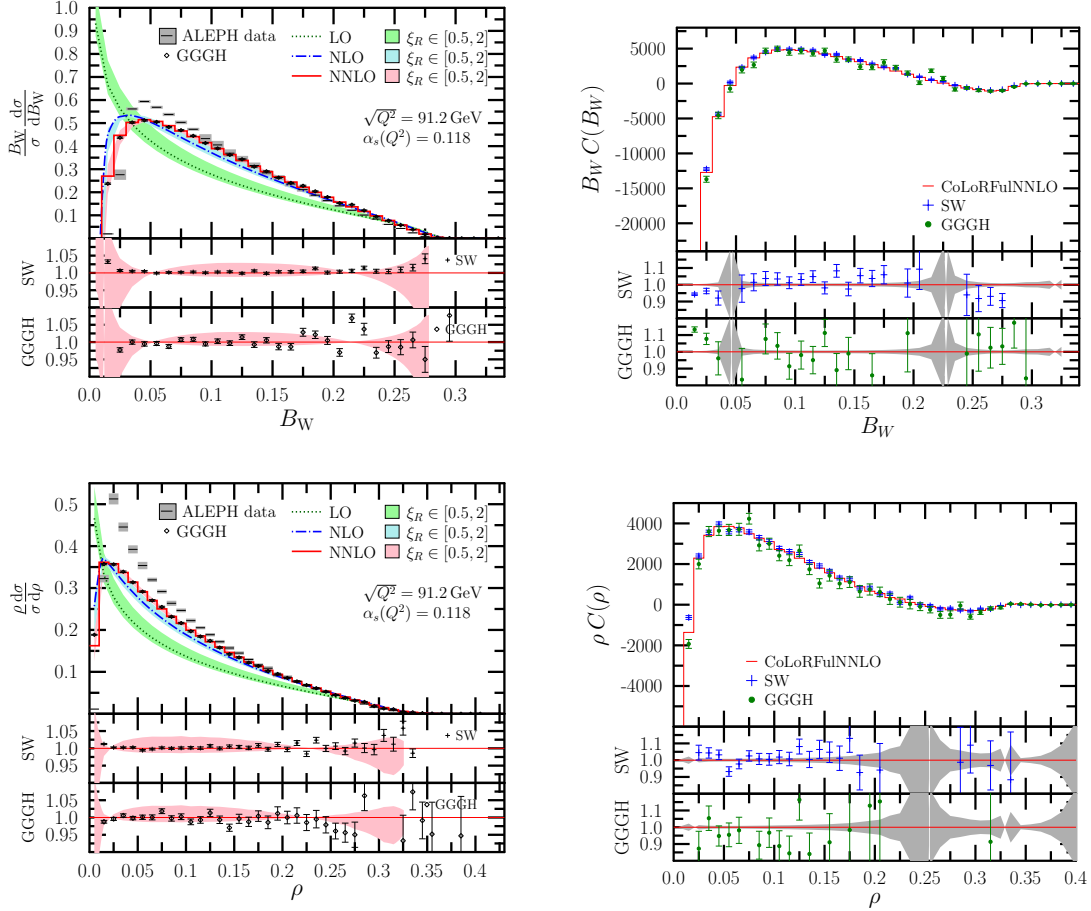


Figure 1: Predictions for the physical and C -coefficient of wide-jet broadening and heavy-jet mass with comparison to [3] (SW) and [2] (GGGH).

We compared our results to previous calculations and found agreement. In our computations we achieved very small statistical uncertainty for all the computed observables demonstrating the robustness of the method and numerical stability of our code.

At present the CoLoRFulNNLO is worked out for colorless initial states. The generalization to partonic initial states is in progress.

References

- [1] S. Becker, D. Goetz, C. Reuschle, C. Schwan and S. Weinzierl, Phys. Rev. Lett. **108**, 032005 (2012) [arXiv:1111.1733 [hep-ph]].
- [2] A. Gehrmann-De Ridder, T. Gehrmann, E. W. N. Glover and G. Heinrich, JHEP **0712**, 094 (2007) [arXiv:0711.4711 [hep-ph]].
- [3] S. Weinzierl, JHEP **0906**, 041 (2009) [arXiv:0904.1077 [hep-ph]].
- [4] G. Somogyi, Z. Trocsanyi and V. Del Duca, JHEP **0701** (2007) 070 [hep-ph/0609042].
- [5] G. Somogyi and Z. Trocsanyi, JHEP **0701** (2007) 052 [hep-ph/0609043].

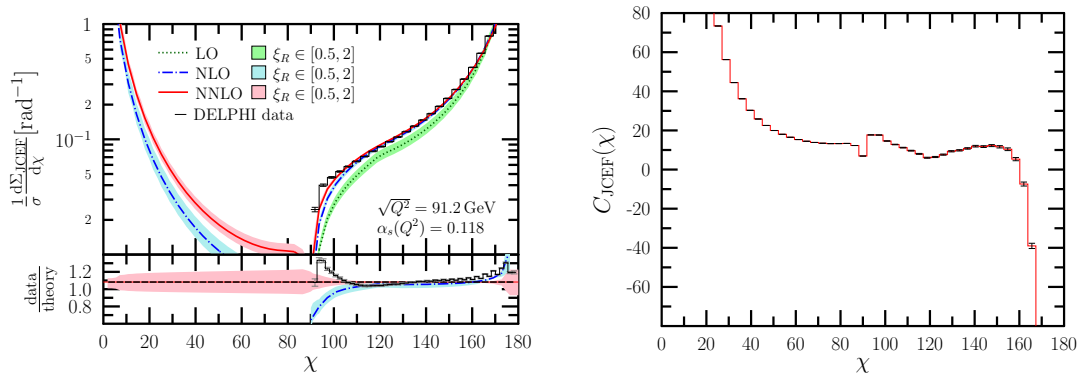


Figure 2: The physical prediction and NNLO QCD correction for the jet cone energy fraction. For the physical prediction the lower panel shows the scale uncertainties as bands and the continuous lines represent the ratio to the NNLO prediction.

- [6] R. Kleiss, W. J. Stirling and S. D. Ellis, *Comput. Phys. Commun.* **40**, 359 (1986).
- [7] C. G. Papadopoulos, *Comput. Phys. Commun.* **137**, 247 (2001) [hep-ph/0007335].
- [8] A. van Hameren, *Acta Phys. Polon. B* **40**, 259 (2009) [arXiv:0710.2448 [hep-ph]].
- [9] P. Nason, arXiv:0709.2085 [hep-ph].
- [10] A. van Hameren, arXiv:1003.4953 [hep-ph].
- [11] S. Platzer, arXiv:1308.2922 [hep-ph].
- [12] J. Alwall *et al.*, *JHEP* **1407**, 079 (2014) [arXiv:1405.0301 [hep-ph]].
- [13] Y. Ohnishi and H. Masuda, “The Jet cone energy fraction in $e^+ e^-$ annihilation,”.